

Compact dimension of denatured states of staphylococcal nuclease

C.-Y. Chow,¹ Ming-Chya Wu,^{1,2} Huey-Jen Fang,³ Chin-Kun Hu,^{1,4} Hueih-Min Chen,^{3,5*} and Tian-Yow Tsong^{6*}

¹Institute of Physics, Academia Sinica, Nankang, Taipei 11529, Taiwan

²Research Center for Adaptive Data Analysis, National Central University, Chungli 32001, Taiwan

³Agricultural Biotechnology Research Center, Academia Sinica, Nankang, Taipei 11529, Taiwan

⁴Department of Physics and Center for Nonlinear and Complex Systems, Chung Yuan Christian University, Chungli 32023, Taiwan

⁵Nano Biosystem Technology Division, National Nano Device Laboratories, Hsinchu 30078, Taiwan

⁶Institute of Physics, Academy of Sciences, Taipei 11529, and National Chiao-Tung University, Hsinchu 30010, Taiwan

ABSTRACT

Fluorescence and circular dichroism stopped-flow have been widely used to determine the kinetics of protein folding including folding rates and possible folding pathways. Yet, these measurements are not able to provide spatial information of protein folding/unfolding. Especially, conformations of denatured states cannot be elaborated in detail. In this study, we apply the method of fluorescence energy transfer with a stopped-flow technique to study global structural changes of the staphylococcal nuclease (SNase) mutant K45C, where lysine 45 is replaced by cysteine, during folding and unfolding. By labeling the thiol group of cysteine with TNB (5,5'-dithiobis-2-nitrobenzoic acid) as an energy acceptor and the tryptophan at position 140 as a donor, distance changes between the acceptor and the donor during folding and unfolding are measured from the efficiency of energy transfer. Results indicate that the denatured states of SNase are highly compact regardless of how the denatured states (pH-induced or GdmCl-induced) are induced. The range of distance changes between two probes is between 25.6 and 25.4 Å while it is 20.4 Å for the native state. Furthermore, the folding process consists of three kinetic phases while the unfolding process is a single phase. These observations agree with our previous sequential model: $N_0 \rightleftharpoons D_1 \rightleftharpoons D_2 \rightleftharpoons D_3$ (Chen et al., *J Mol Biol* 1991;220:771–778). The efficiency of protein folding may be attributed to initiating the folding process from these compact denatured structures.

Proteins 2008; 72:901–909.
© 2008 Wiley-Liss, Inc.

Key words: staphylococcal nuclease; differential scanning microcalorimetry; fluorescence energy transfer; denatured state; folding kinetics.

INTRODUCTION

The mechanism of protein folding and unfolding is an important unsolved problem in biological science. Understanding the details of protein folding will be helpful in the design of novel proteins with specific structures and functions,¹ which are useful in biomedical science or protein biotechnology. To determine the mechanisms of folding/unfolding, one should try to identify intermediates that define and direct the pathway. Since the intermediate states are usually thermodynamically unstable and hardly observed, a number of techniques such as stopped-flow kinetics and differential scanning microcalorimetry (DSC) have been employed to determine rates and possible pathways of protein folding.^{2–4} However, a complete description of protein kinetics requires three variables: time scales, amplitudes, and spatial extent.⁵ The methods mentioned above cannot completely determine all of these parameters, especially the spatial information of protein in folding/unfolding. Without detailed information of protein denatured state,^{6–11} the whole folding/unfolding processes would not be solved completely even the protein native state might have been well defined.

To understand protein conformations in the denatured states, in this article, we use the methods of fluorescence stopped-flow kinetics and efficiency of energy transfer (EET)^{12–14} to monitor

Abbreviations: DSC, differential scanning microcalorimetry; EET, efficiency of energy transfer; RD, relative distance; SNase, staphylococcal nuclease; TNB, 5,5'-dithiobis-2-nitrobenzoic acid.

Grant sponsor: National Science Council, Taiwan, R.O.C.; Grant numbers: NSC 95-2320-B-001-019, NSC 95-2112-M-001-008, NSC 96-2112-M-008-021-MY3; Grant sponsors: National Center for Theoretical Sciences in Taiwan; Thematic Project AS-95-TP-A07 of Academia Sinica (Taipei).

*Correspondence to: Dr. T.-Y. Tsong, Institute of Physics, Academy of Sciences, Taipei 11529, Taiwan. E-mail: tsongty@phys.sinica.edu.tw or tsong001@umn.edu; or Dr. H.-M. Chen, Nano Biosystem Technology Division, National Nano Device Laboratories, Hsinchu 30010, Taiwan. E-mail: robell21@yahoo.com

Received 13 June 2007; Revised 6 December 2007; Accepted 28 December 2007

Published online 14 February 2008 in Wiley InterScience (www.interscience.wiley.com).

DOI: 10.1002/prot.21985

the distance changes between donor (tryptophan at position 140 as a donor) and acceptor (cysteine at position 45 modified with TNB, 5,5'-dithiobis-2-nitrobenzoic acid, as an acceptor) in the staphylococcal nuclease (SNase)¹⁵ mutant K45C, where lysine 45 is replaced by a cysteine. During protein unfolding, the distance between two positions varies with conformational changes. By measuring of the EET, we can determine the distances between two probes at different stages of folding/unfolding and estimate the dimension of denatured states.

SNase is a small single-domain protein with 149 amino acids and without disulfide bonds.¹⁵ It has no cysteine and includes only one tryptophan at position 140, which makes it as a good model protein. For the kinetics of SNase folding, previous reports^{16,17} by using fluorescence stopped-flow showed that the refolding of acid-induced unfolded SNase is a two-step process. The faster step (50 ms) is a nucleation process and the slow step (550 ms) is the main folding process. Furthermore, there is an additional slower step (35 s) corresponding to proline isomerization.¹⁸ Our previous report⁴ has identified the three processes and proposed a model of "least activation path" in which the whole folding process consists of three denatured states and one native state: $N_0 \rightleftharpoons D_1 \rightleftharpoons D_2 \rightleftharpoons D_3$, where N_0 indicates a native state and D_i 's are denatured states. For these "kinetic" denatured states, many studies^{10,11,19,20} have shown that denatured states are compact if the protein is mildly denatured. For example, Wu and Brand^{21,22} used fluorescence energy transfer to study the distance between Cys-78 and Trp-140 of SNase mutant K78C and reported that it is about 25 Å. However, their experiments were conducted in the "static" environment (denatured state at equilibrium), in which only the denatured state D_3 can be studied.⁴

In this study, we use fluorescence stopped-flow kinetics and EET¹⁴ to measure fluorescence energy transfer and determine the distances between W140 and K45C in the denatured states of K45C mutant. For the first time, these measurements are done in a "dynamic" environment, which uniquely provide useful information about the sequential changes of the dimension of the protein in the denatured states. Based on the obtained results, we propose a clear scheme of SNase folding/unfolding.

METHODS

Materials

Wild-type (WT) SNase *nuc* gene was originally donated by Prof. David Shortle. Luria-Bertani broth and isopropyl-1-thio-β-D-galactopyranoside were purchased from Difco Laboratories and Sigma, respectively. Salmon testes DNA and some analytical grade chemicals such as EDTA, Tris-HCl, CaCl₂, NaCl, and mineral oil were obtained from Sigma. Salmon testes DNA was used without further purification. Guanidine hydrochloride and dNTPs

were purchased from Roche Molecular Bio-chemicals. Absolute ethanol (>99%) was obtained from Panreac and urea was a product of Acros. The Stratagene Quick-ChangeTM kit containing *Pfu* DNA polymerase, 10× reaction buffer and *DpnI* restriction enzyme was purchased from Stratagene. The 2-methyl-2,4-pentadiol was purchased from Merck. Water used for these experiments has been deionized and distilled.

Sample preparation

Mutant K45C was generated by ExSiteTM (Stratagene) PCR-based site-directed mutagenesis. The detailed procedures followed Ref. 23. Both WT and mutant proteins were purified as described in Ref. 24. The purity of protein was checked and found to be higher than 90%. K45C mutant was labeled as follow^{21,22}: free thiol or oxidized disulfide K45C was dissolved in a buffer containing 0.1M Tris, 0.05M NaCl, and 1 mM EDTA at pH 8.0. Reduction of disulfide bond was achieved by adding 500-fold excess of dithiothreitol (DTT) and stored in 60°C for 2 h. Excessive DTT was removed by Pharmacia PD-10 desalting column. TNB in 100-fold excess was added to the protein in the same buffer. The reaction mixture was stirred in the dark for 2 h. Excessive TNB was removed by PD-10 column. The protein was further purified by HPLC gel filtration column and the final product was dissolved in a 50 mM phosphate buffer at pH 7.0. The labeling ratio was measured²⁵ and found to be 1.03.

Fluorescence energy transfer measurements

Fluorescence energy transfer is the transfer of electronic energy between a fluorescent donor and an acceptor.^{13,26} According to the Förster's theory,²⁷ the rate of energy transfer (k_T) is proportional to the inverse sixth power of the distance between the donor and the acceptor:

$$k_T = r^{-6} K^2 n^{-4} k_F J \times 8.71 \times 10^{23} \text{ s}^{-1} \quad (1)$$

where r is the distance between the donor and the acceptor, K is the orientation factor for a dipole-dipole interaction, n is the refractive index of the medium between the donor and the acceptor, k_F indicates the rate constant of donor's fluorescence emission, and J indicates the spectral overlap integral defined by:

$$J = \int F_D(\lambda) \epsilon_A(\lambda) \lambda^4 d\lambda \quad (2)$$

where $F_D(\lambda)$ is the peak-normalized fluorescence spectrum of the donor at wavelength λ and ϵ_A is the acceptor molar absorption. The EET can be calculated by using the following equation:

$$E = r^{-6} / (r^{-6} + R_0^{-6}) \quad (3)$$

where R_0 is the distance at which the EET is 50% and can be further calculated by the following equation²⁸:

$$R_0 = (JK^2Q_0n^{-4})^{1/6} \times 9.7 \times 10^3 \text{ \AA} \quad (4)$$

where Q_0 indicates the quantum yield of donor's fluorescence in the absence of acceptor.

Circular dichroism measurements

Circular dichroism (CD) spectra of SNase at different pH and [GdmCl] were measured (200–250 nm) with a Jasco (Easton, MD) J-720 spectropolarimeter. Water-jacketed quartz cell with light path of 1 mm was used. The protein samples were kept at 1 mg/mL in a 50 mM phosphate buffer. To prevent thiol oxidation, DTT 0.5 mM was added in the unlabeled K45C sample. Data below 200 nm was not recorded because of the interference from DTT. Analysis of CD spectra was done according to the procedure of Chang *et al.*²⁹ The folding/unfolding reactions were monitored by CD at 222 nm as a function of pH or [GdmCl]. The molar ellipticity was calculated using an average molecular weight per amino acid residue of 112.5 Da.

Calorimetry measurements

DSC was performed with a model N-DSC by Calorimetry Sciences Corp. The cell volume was around 0.5 mL and the scanning rate was 1 K/min. Protein concentrations of 1–3 mg/mL were used and the sample was kept in a 50 mM phosphate buffer at pH 7.0 including 0.5 mM DTT. Data analysis followed Ref. 30.

Steady-state fluorescence measurements

Steady-state fluorescence measurements were performed on a Perkin-Elmer LS50B Luminescence spectrometer with a 1.0 cm × 1.0 cm quartz fluorescence cuvette. Both pH (1.5–11.0; 0.2–0.5 pH increments) and GdmCl (0M to 2.0M with increments of 0.2M to 0.5M; at pH 7.0) denaturations of labeled and unlabeled K45C were performed at 25°C. The protein concentration used was at 0.1 mg/mL in a 50 mM phosphate buffer. The excitation beam was set at 285 nm. Both original and corrected emission spectra were recorded for the transformation into EET and relative distances (RD; or called Förster distance). Each measurement was repeated five times at a given condition to ensure reproducibility.

Stopped-flow measurements

Stopped-flow fluorescence was performed with model SX.17MV stopped-flow reaction analyzer with CD detectors from Applied Photophysics (Leatherhead, UK). The

dead mixing time was 0.8 ms and the kinetic measurements between 2 ms and 300 s can be measured with confidence. The excitation beam was set at 285 nm and the integrated fluorescence larger than 300 nm was recorded as a function of time. Both pH- and GdmCl-induced folding/unfolding experiments were done: (i) pH-induced refolding experiment: proteins at pH 2 (0.1 mg/mL with 10 mM sodium acetate, potassium phosphate and glycine) was mixed with 10 volumes of the same buffer at pH 7.1 so that the pH of the protein sample was brought to the final pH 7.0; (ii) pH-induced unfolding experiment: the starting protein sample was set at pH 7.0 and the final pH of the sample was 2.0; (iii) GdmCl-induced refolding experiment: about 0.1 mg/mL of protein was dissolved in a 10 mM phosphate buffer at pH 7.0 with 2.0M GdmCl. A single jump stopped-flow was performed. Afterwards, the final GdmCl concentration was reduced to 0.2M; (iv) GdmCl-induced unfolding experiment: the concentration of GdmCl was increased from 0.2 to 2.0 M. Each experimental data to be reported below was an average of five independent measurements. In our previous study of the tryptophan fluorescence of SNase at pH 2.8, 7.0, and 11.6 as a function of protein concentration,³¹ results show that SNase at these pH values does not aggregate in a protein concentration below 70 μM (1.18 mg/mL). In the present study, protein concentration has been carefully controlled below this threshold such that aggregation can be ruled out as a possible source of intermediates.

RESULTS

Characteristics of labeled protein K45C-TNB and unlabeled protein K45C

The thermal characteristics and secondary structures of SNase and its mutant K45C were investigated by DSC and CD, respectively. The thermal parameters of melting point (T_m), heat capacity change (ΔC_p), and enthalpy change (ΔH) were measured and $T_m = 53.1/52.4/51.7^\circ\text{C}$, $\Delta C_p = 2.32/2.28/2.49 \text{ kcal/mol}$, and $\Delta H = 85.3/82.3/76.2 \text{ kcal/mol}$ for WT, K45C, and K45C-TNB, respectively. The results show that all the three proteins have similar thermal stability, but the ΔH of K45C-TNB is relatively lower. Similar CD spectra of the three proteins imply that they have similar secondary structures. The acid-induced conformational changes of K45C and K45C-TNB proteins followed the change of pH (pH 1 to pH 9) in fluorescence measurements. The fluorescence is largely quenched by labeling TNB to cystein in K45C. The mid-point transitions of K45C and K45C-TNB were at pH 3.9 and 4.1, respectively. These observations imply that point mutation or addition of TNB to the protein at position 45 alters very little its characteristics including stability and conformation.

Table I

Distances Between Trp-140 and Cys-TNB-45 in Different Protein States

Condition	E'	RD (Å)
0.2M GdmCl, pH 7.0	0.761 ± 0.002	20.35 ± 0.04
2.0M GdmCl, pH 2.0	0.416 ± 0.006	25.39 ± 0.10
pH 7.0, no GdmCl	0.733 ± 0.002	20.28 ± 0.06
pH 2.0, no GdmCl	0.402 ± 0.008	25.56 ± 0.15

The efficiency of energy transfer (E') and RD (Å) for protein at different states were shown. Each measurement was repeated for 20 times and the experiments were done at room temperature.

Distances between Cys-TNB-45 and Trp-140 in native and denatured states of K45C-TNB

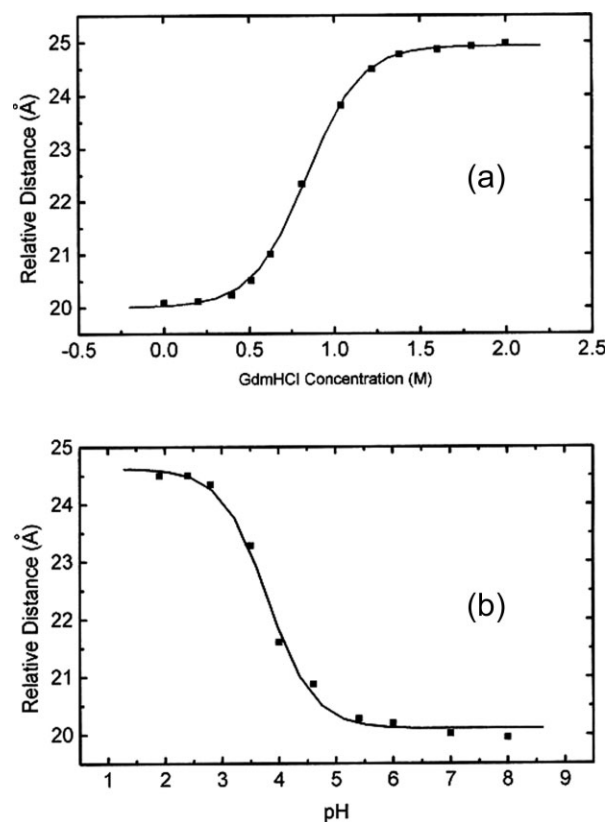
Both labeled and unlabeled proteins were investigated by the steady-state fluorescence. The empirical EET (E') can be calculated from the difference of intensity of tryptophan fluorescence between labeled K45C-TNB and unlabeled K45C proteins at the same condition:

$$E' = 1 - \langle \tau_{DA} \rangle / \langle \tau_D \rangle \quad (5)$$

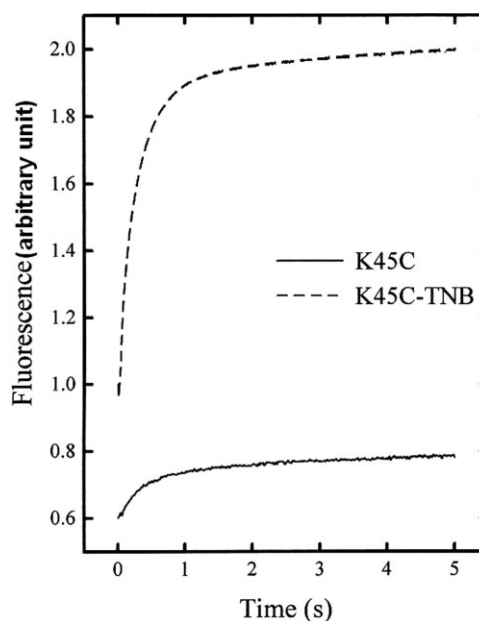
where τ_{DA} is the intensity of tryptophan fluorescence of labeled protein and τ_D is the intensity of tryptophan fluorescence of unlabeled protein. The RD between two fluorescence probes is obtained by the Förster equation:

$$r = R_0 [1 / (E' - 1)]^{1/6} \quad (6)$$

Both results of E' and RD in different protein states are summarized in Table I. For protein in native state, the RD is about 20.4 Å as compared with the protein in denatured states where the RD is ranged from 20.3–25.6 Å. Note that the RD of WT SNase, measured by the X-ray crystallography,³² is 21.5 Å. Lys45 is in a very flexible loop. The minor difference in the RD measurements by EET and X-ray (± 1.1 Å or 5% in deviation) might be due to different states used: the former is in a solution state, while the latter is in a solid state. More details were done (see Fig. 1) for the changes of the RD between Cys-TNB-45 and Trp-140 during GdmCl [Fig. 1(a)] and pH [Fig. 1(b)] titration. The RD of Cys45-TNB and Trp-140 in denatured states (both GdmCl and acid denatured states) is again ranged from 20–25 Å.

**Figure 1**

Distance measurements among proteins at different states. The distances between Trp-140 and Cys-TNB-45 were measured by the EET with the following different initial conditions: (a) GdmCl induced denaturation from 0.2M GdmCl to 2.0M GdmCl (pH was fixed at 7.0) and (b) pH-induced denaturation from pH 7.0 to pH 2.0 (without the addition of GdmCl).

**Figure 2**

Typical fluorescence refolding curves of K45C and K45C-TNB. The initial condition of denatured states of both K45C and K45C-TNB was in a buffer with 2.0M GdmCl. The curves of EET and relative distances shown in Figures 3–6 were transformed according to the typical curves shown here.

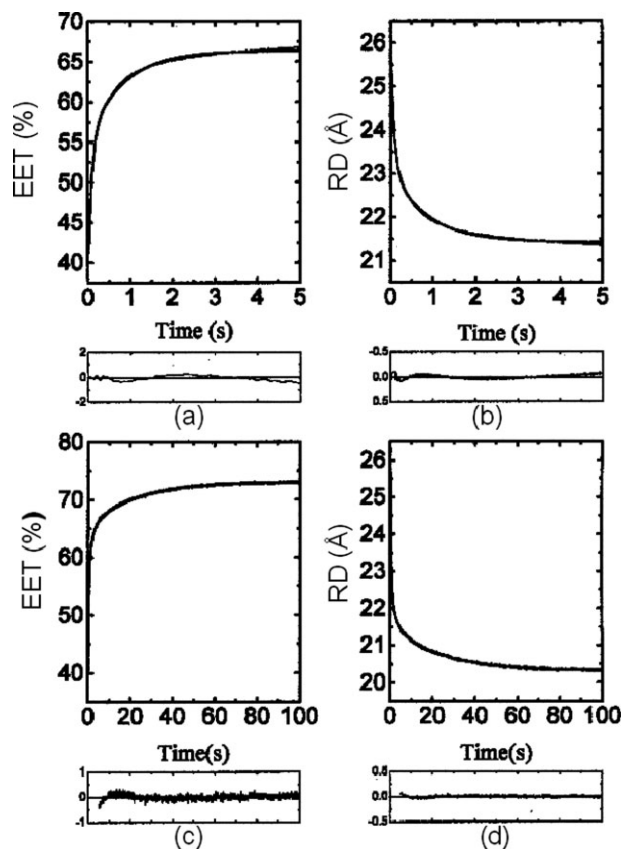


Figure 3

pH refolding kinetics of K45C-TNB. The initial condition of denatured state of K45C was in a buffer at pH 2. The refolding kinetics experiment was done (from pH 2 to pH 7) by two time scales: 0–5 s as shown in (a) for EET changes and (b) for relative distance changes; 0–100 s as shown in (c) for EET changes and (d) for relative distance changes.

Kinetics of protein folding/unfolding

The folding processes of denatured proteins were induced by changing either pH (pH 2.0 to pH 7.0) or GdmCl (2.0–0.2M). Folding kinetics of the labeled proteins was monitored by Trp fluorescence using stopped-flow method. Typical kinetic fluorescence curves of labeled and unlabeled proteins are shown in Figure 2. Both EET and RD kinetic curves were obtained from Eqs. (5) and (6) by using the data of Figure 2, for example. Figures 3 and 4 show pH refolding and unfolding kinetic curves for both EET and RD, respectively. The refolding kinetics experiments were done by two time scales: 0–5 s and 0–100 s, and the unfolding kinetics experiments were done within a time scale of 0–5 s. Figures 5 and 6 show GdmCl refolding and unfolding kinetic curves for both EET and RD, respectively. The refolding kinetics experiments were done by two time scales: 0–5 s and 0–200 s, and the unfolding kinetics experiments were done within a time scale of 0–20 s. Following the approach of

folding proposed by Chen *et al.*,³³ we fitted the experimental data in some time range with a single exponentially decay function. The boxes below the graphs indicate residuals of the fit. For the refolding reactions, the curves for EET and RD can be, respectively, fitted by three exponential terms: two for the shorter time scale between 2 ms and 5 s, and one for a longer time scale (5–100 s for pH-induced refolding or 5–200 s for GdmCl-induced refolding). Three kinetic phases were therefore observed during protein refolding, while one kinetic phase was obtained for protein unfolding. The detailed kinetic results are shown in Tables II and III for pH-induced and GdmCl-induced refolding/unfolding, respectively.

DISCUSSION

The folding kinetics for K45C monitored by the RD between Trp-140 and Cys-TNB-45 is very similar to that for the WT SNase monitored by Trp-140 fluorescence.^{4,14} Both of them have three kinetic phases of refolding and one phase of unfolding.⁴ Possible folding models may include parallel and sequential folding pathways. However, our previous stopped-flow kinetic measurements³³ show that three substates have similar enthalpy and tryptophan fluorescence and their equilibrium cannot be shifted by temperature changes. These substates are distinguished by the kinetic barriers among them, and their state differences are purely entropic.³³ The experimental observations of no difference between van't Hoff enthalpy change and calorimetric value ($\Delta H_{VH} = \Delta H_{cal}$) and two-state-like transition exclude parallel

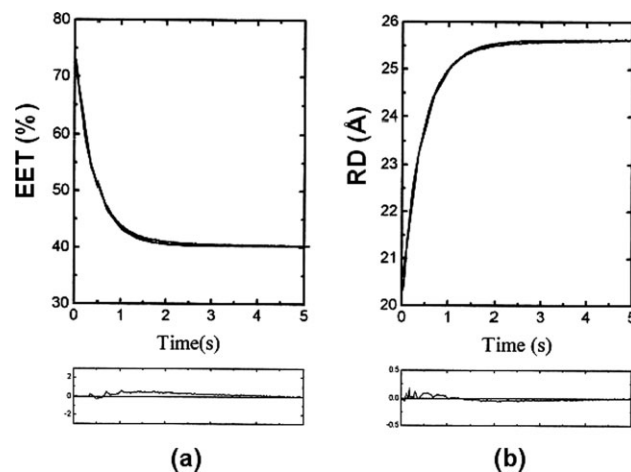


Figure 4

pH unfolding kinetics of K45C-TNB. The initial condition of native state of K45C was in a buffer at pH 7. The unfolding kinetics experiment was done (from pH 7 to pH 2) within a time scale of 0–5 s as shown in (a) for EET changes and (b) for relative distance changes.

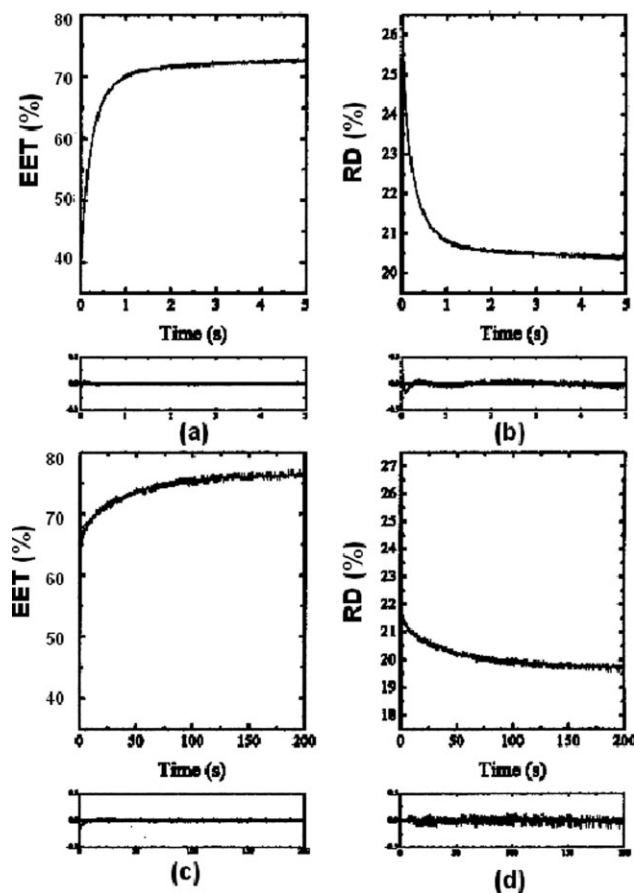


Figure 5

GdmCl refolding kinetics of K45C-TNB. The initial condition of denatured state of K45C was in a buffer with 2M GdmCl. The refolding kinetics experiments was done (from 2M GdmCl to 0.2M GdmCl) in two time scales: 0–5 s as shown in (a) for EET changes and (b) for relative distance changes; 0–200 s as shown in (c) for EET changes and (d) for relative distance changes.

folding pathways, and agree with the sequential model.^{4,33} We then proposed the pathways of folding/unfolding as follows^{4,31,33–35}: pH-induced folding/unfolding pathway: $D_3 \rightleftharpoons D_2 \rightleftharpoons D_1 \rightleftharpoons N_0$; GdmCl-induced folding/unfolding pathway: $U_3 \rightleftharpoons U_2 \rightleftharpoons U_1 \rightleftharpoons N_0$, where D_i and U_i represent the denatured state and N_0 is the native state. Note that even though there are three phases in folding kinetics, only N_0 and D_3 (or U_3) can be observed in equilibrium. Su *et al.*⁴ showed that the activation energy among three denatured states are small (~ 0.5 kcal/mol) such that conversions among these substates do not involve significant changes of free energy. Similar results have been obtained from general fluorescence and CD kinetic experiments.⁴

According to our RD measurements, the distances between Trp-140 and Cys-TNB-45 in K45C were 22.8, 25.4, and 25.6 Å for D_1 , D_2 , and D_3 , respectively and 22.8, 24.2, and 25.4 Å for U_1 , U_2 , and U_3 , respectively

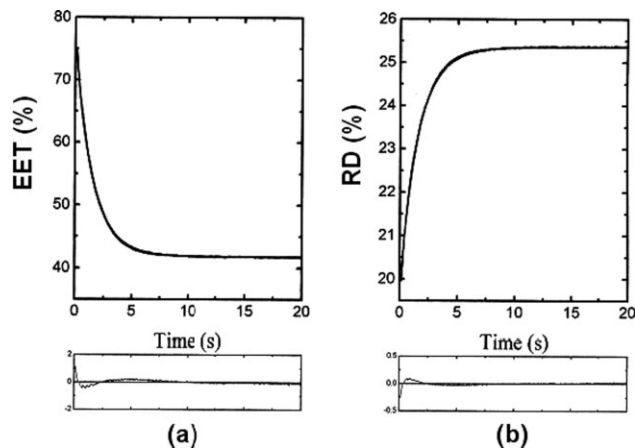


Figure 6

GdmCl unfolding kinetics of K45C-TNB. The initial condition of native state of K45C was in a buffer with 0.2M GdmCl. The unfolding kinetics experiment was done (from 0.2M GdmCl to 2M GdmCl) within a time scale of 0–20 s as shown in (a) for EET changes and (b) for relative distance changes.

(see Tables II and III for details). The RDs of D_1 (22.8 Å) and U_1 (22.8 Å) are the shortest, and the differences of the RDs of D_2 (25.4 Å), D_3 (25.6 Å) and U_2 (24.2 Å), U_3 (25.4 Å) with respect to that of the native state (20.4 Å) are roughly the amplitude of fluctuation (± 5 Å) of the TNB group attached to K45C.²² Note that the gyration radius of the native state SNase evaluated from PDB (Protein Data Bank)³⁶ data 1EY0.pdb is 13.48 Å, and the dimension of the native conformation has a radius of 26.47 Å. Even though SNase protein does not behave like an ideal statistical polymer chain,⁴ we can evaluate its properties from comparing its PDB structure with a random polypeptide. According to the statistical properties of random polypeptides, the average gyration radius $\langle R_G \rangle$ and the average end-to-end distance r of a random-flight chain separated by l bonds is given by³⁷

$$\langle R_G \rangle^2 = (\langle r^2 \rangle / 6)(l + 2) / (l + 1). \quad (7)$$

The native state of SNase has an end-to-end distance of 36.76 Å, measured from K6 to S141 (i.e., $l = 135$), and $\langle R_G \rangle = 15.06$ Å which is smaller than a random coil

Table II

Kinetics of pH-Induced Folding/Unfolding of K45C-TNB

Reaction	Relaxation time	Amplitude (%)	EET (%)	RD (Å)
Unfolding from pH7.0 to pH2.0				
$N_0 \rightarrow D_3$	0.42 s	100	73.3% → 40.2%	20.4 → 25.6 (5.2)
Folding from pH2.0 to pH7.0				
$D_1 \rightarrow N_0$	80 ms	56	58.7% → 40.2%	22.8 → 20.4 (2.4)
$D_2 \rightarrow D_1$	830 ms	39.9	72.0% → 58.7%	24.5 → 22.8 (1.7)
$D_3 \rightarrow D_2$	20.67 s	4.1	73.3% → 72.0%	25.6 → 24.5 (1.1)

Table III

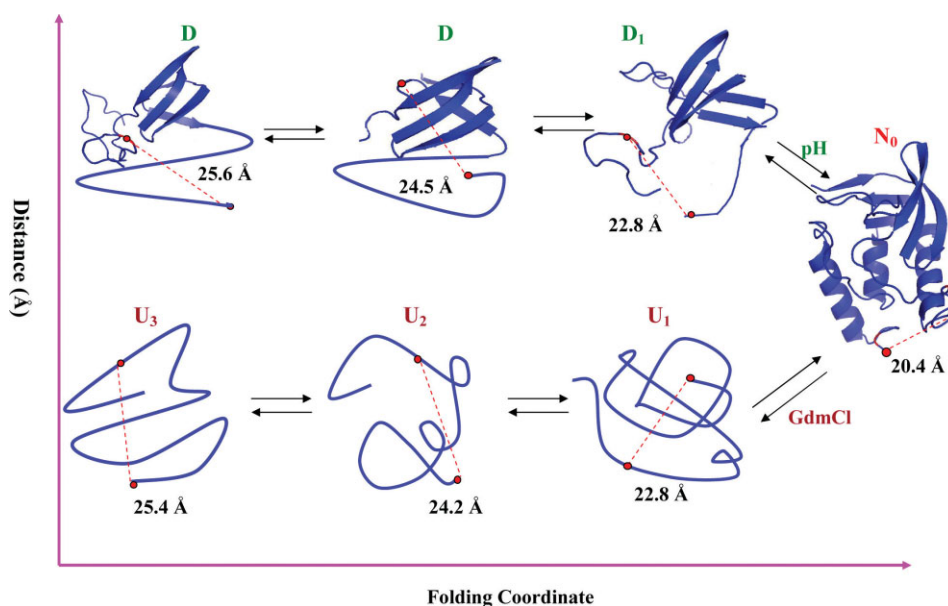
Kinetics of GdmCl-Induced Folding/Unfolding of K45C-TNB

Reaction	Relaxation time	Amplitude (%)	EET (%)	RD (Å)
Unfolding from 0M GdmCl to 2.0M GdmCl				
$N_0 \rightarrow U_3$	1.51 s	100	76.2% → 41.6%	20.3 → 25.4 (5.1)
Folding from 2.0M GdmCl to 0.2M GdmCl				
$U_1 \rightarrow N_0$	186 ms	68.2	65.2% → 41.6%	22.8 → 20.3 (2.5)
$U_2 \rightarrow U_1$	806 ms	13.0	69.7% → 65.2%	24.2 → 22.8 (1.4)
$U_3 \rightarrow U_2$	43.88 s	18.8	76.2% → 69.5%	25.4 → 24.2 (1.2)

conformation ($\langle R_G \rangle \approx 40 \text{ \AA}$) and is larger than a sphere-like structure ($\langle R_G \rangle \approx 13 \text{ \AA}$).³⁷ This implies that SNase is essentially a compact protein. For denatured states, we follow the same scheme to infer the corresponding dimensions. Since there is no structure determination for denatured states of K45C, we evaluate their compactness by the end-to-end distance from K45C to W140 (i.e., $l = 95$) instead of K6 to S141. For the native state of K45C, the end-to-end distance is $r = 21.46 \text{ \AA}$, and $\langle R_G \rangle = 8.81 \text{ \AA}$ which is smaller than a random coil conformation ($\langle R_G \rangle \approx 34 \text{ \AA}$) and a sphere-like structure ($\langle R_G \rangle \approx 11 \text{ \AA}$). For the denatured states of K45C, the largest end-to-end distance from K45C to W140 is $r = 25.6 \text{ \AA}$ and $\langle R_G \rangle = 10.51 \text{ \AA}$ which is still smaller than a random coil con-

formation ($\langle R_G \rangle \approx 34 \text{ \AA}$) and is similar to a sphere-like structure ($\langle R_G \rangle \approx 11 \text{ \AA}$). All of these suggest that the dimensions of denatured states D_1 , D_2 , and D_3 , and U_1 , U_2 , and U_3 of K45C remain in very similar size scale as that of the native protein, and D_i might even maintain a native-frame-based conformation (CD measurements indicate there are secondary structures in D_i , mainly β -sheets; while there is no secondary structure in U_i . See Figure 1(b) of Ref. 33), similar to that reported in Ref. 38. According to these observations and reports in existing studies,^{4,22,31,33,38–41} the denatured states appear to be compact and essentially disordered,^{33,42} as illustrated schematically in Figure 7. In a typical cluster model of protein folding,⁴³ (Wu *et al.*, manuscript submitted) hydrophobic condensation may cause a polypeptide to form a molten globule,⁴⁴ resembling to the compact denatured structures^{45,46} considered here, which is followed by folding process involves formation of hydrogen bonds of secondary structures and stabilization of these structures.^{47,48} (Wu *et al.*, manuscript submitted) Denaturation substantially follows an inverse sequence.

Recent solution structural study⁴⁹ on the mutant (L16A) of *Drosophila Melanogaster* Engrailed homeodomain (En-HD) showed that both intermediate and denatured states are experimentally indistinguishable. The denatured state of En-HD could be defined from its mutant L16A by varying the ionic strength. Our D_1 (or U_1) state in SNase could be considered as a state between

**Figure 7**

Schematic representation of native and denatured states of SNase induced by the changes of pH and GdmCl. At pH 7 and 25°C with no GdmCl or with GdmCl < 0.2M, the protein exists in the N_0 state. The distance between Trp140 and Cys45 (red dots) is about 20.4 Å. D_1 , D_2 , and D_3 represent the denatured states at pH 2 and U_1 , U_2 , and U_3 indicated the denatured states at 2M GdmCl (the scheme is adapted from Ref. 4). The structure of SNase at native state was plotted according to the PDB structure 1EY0.pdb.

folded and denatured states. Further report concerning the denatured states of SNase was presented by Sallum *et al.*,⁵⁰ who used NMR residual dipolar couplings to propose that the conformation of a denatured SNase favors the disruption of cooperative structure, but not the retention of a unique long-range folding topology. If this is the case, based on our RD measurements for the denatured states, we would propose that these disruptive conformations are within a constraint dimension, but not in the case of free expansion. These denatured states are in compact forms as the native state. The similar dimension between native and denatured states (especially D_1 or U_1 state) might have the latter in a “ready” condition to efficiently refold. The efficiency of protein folding is only in the case of D_1 (or U_1) toward N_0 . *In vivo*, we would image that the protein (such as SNase) folding after secreting from ribosomes may start from a compact conformation such as D_1 or U_1 . The random linear conformation (not in the compact form) of proteins in solution (regardless they are *in vitro* or *in vivo*) may not exist.

Finally, we would emphasize that the measurement of the average RD in denatured states by the Förster theory involves an uncertainty from the average of a heterogeneous ensemble of denatured conformations. For a Gaussian distribution of distances of denatured conformations, this uncertainty is roughly in a linear relation with mid-width of the distribution, according to Eq. (6). Thus, for the distribution with a mid-width of 2α , the uncertainty is about α . As mentioned above, Lys45 is in a flexible loop and the flexibility contributes the fluctuation amplitude of 5 Å to the RD measurements. Consequently, the average RD is the most probable separation of two probes in our study, while the deviation contributed by a long separation can be up to 25%. The development of new techniques for the refinement of the distance determination is therefore required. We are working in this direction and will report our results in near future.

REFERENCES

- Chan H-S, Dill KA. The protein folding problem. *Phys Today* 1993; 46:24–32.
- Tsong T-Y. The Trp-59 fluorescence of ferricytochrome c as a sensitive measure of the over-all protein conformation. *J Biol Chem* 1974; 249:1988–1990.
- Tsong T-Y. Ferricytochrome c chain folding measured by the energy transfer of tryptophan 59 to the heme group. *Biochemistry* 1976;15: 5467–5473.
- Su ZD, Arooz TM, Chen HM, Gross CJ, Tsong TY. Least activation path for protein folding: investigation of staphylococcal nuclease folding by stopped-flow CD. *Proc Natl Acad Sci USA* 1996;93:2539–2544.
- McCammon JA, Harvey SC. Dynamics of protein and nucleic acids. New York: Cambridge University Press; 1987.
- Gillespie JR, Shortle D. Characterization of long-range structure in the denatured state of staphylococcal nuclease. II. Distance restraint from paramagnetic relaxation and calculation of an ensemble of structures. *J Mol Biol* 1997;268:170–184.
- Yi Q, Kim S, Alm EJ, Baker D. NMR characterization of residual structure in the denatured state of protein L. *J Mol Biol* 2000;299: 1341–1351.
- Lietzow MA, Jamin M, Dyson HJJ, Wright PE. Mapping long-range contacts in a highly unfolded protein. *J Mol Biol* 2002;322:655–662.
- Teilmann K, Kragelund BB, Poulsen FM. Transient structure formation in unfolded acyl-coenzyme A-binding protein observed by site-directed spin labeling in 8M urea. *J Mol Biol* 2002;324:349–357.
- Ackerman MS, Shortle D. Molecular alignment of denatured states of staphylococcal nuclease with strained polyacrylamide gels and surfactant liquid crystalline phase. *Biochemistry* 2002;41:3089–3095.
- Ackerman MS, Shortle D. Robustness of the long-range structure in denatured staphylococcal nuclease to changes in amino acid sequence. *Biochemistry* 2002;41:13791–13797.
- Haas E, Wilchek M, Katchalski-Katzir E, Steinberg IZ. Distribution of end-to-end distances of oligopeptides in solution as estimated by energy transfer. *Proc Nat Acad Sci USA* 1975;72:1807–1811.
- Stryer L. Fluorescence energy transfer as a spectroscopic ruler. *Annu Rev Biochem* 1978;47:819–846.
- Chow CY, Tsong T-Y. Folding kinetics of staphylococcus nuclease monitoring relative distance between TRP140 and a fluorophore at position 45. *FASEB J* 1997;11:262.
- Cotton FA, Hazen EE, Legg MJ. Staphylococcal nuclease: proposed mechanism of action based on structure of enzyme-thymidine 3', 5'-bisphosphate-calcium ion complex at 1.5-Å resolution. *Proc Natl Acad Sci USA* 1979;76:2551–2562.
- Schechter AN, Chen RF, Anfinsen CB. Kinetics of folding of staphylococcal nuclease. *Science* 1970;167:886–887.
- Epstein HF, Schechter AN, Chen RF, Anfinsen CB. Folding of staphylococcal nuclease: kinetic studies of two processes in acid renaturation. *J Mol Biol* 1971;60:499–508.
- Davis A, Parr GR, Taniuchi H. A kinetic study of the folding of nuclease B: a possible precursor of staphylococcal nuclease A. *Biochim Biophys Acta* 1979;578:505–510.
- Shortle D, Meeker AK. Residual structure in large fragments of staphylococcal nuclease: Effects of amino acid substitutions. *Biochemistry* 1989;28:936–944.
- Gottfried DS, Hass E. Nonlocal interactions stabilize compact folding intermediates in reduced unfolded bovine pancreatic trypsin-inhibitor. *Biochemistry* 1992;31:12353–12362.
- Wu PG, Brand L. Resonance energy transfer: methods and applications. *Anal Biochem* 1994;218:1–13.
- Wu PG, Brand L. Conformational flexibility in a staphylococcal nuclease mutant K45C from time-resolved resonance energy transfer measurements. *Biochemistry* 1994;33:10457–10462.
- Leung KW, Liaw YC, Chan SC, Lo HY, Musayev FN, Chen JZW, Fang HJ, Chen HM. Significance of local electrostatic interactions in staphylococcal nuclease studies by site-directed mutagenesis. *J Biol Chem* 2001;276:46039–46045.
- Chen HM, Chan SC, Leung KW, Wu JM, Fang HJ, Tsong TY. Local stability identification and the role of key acidic amino acid residues in staphylococcal nuclease unfolding. *FEBS J* 2005;272:3967–3974.
- Riddles PW, Blakeley RL, Zerner B. Ellman's reagent: 5,5'-dithiobis(2-nitrobenzoic acid)—a reexamination. *Anal Biochem* 1979;94:75–81.
- Steinberg IZ. Long-range nonradiative transfer of electronic excitation energy in proteins and polypeptides. *Annu Rev Biochem* 1971; 40:83–114.
- Förster T. Intermolecular energy migration and fluorescence. *Ann Phys* 1948;2:55–75.
- Stryer L, Haugland RP. Energy transfer: a spectroscopic ruler. *Proc Natl Acad Sci USA* 1967;58:719–726.
- Chang CT, Wu CS, Yang JT. Circular dichroic analysis of protein conformation: inclusion of the β -turns. *Anal Biochem* 1978;91:13–31.
- Griko YV, Privalov PL, Sturtevant JM, Venyaminov SY. Cold denaturation of staphylococcal nuclease. *Proc Natl Acad Sci USA* 1988; 85:3343–3347.

31. Chen HM, Markin VS, Tsong TY. pH induced folding/unfolding of staphylococcal nuclease: determination of kinetic parameters by the sequential jump method. *Biochemistry* 1992;31:1483–1491.
32. Chen J, Lu Z, Sakon J, Stites WE. Increasing the thermostability of staphylococcal nuclease: implications for the origin of protein thermostability. *J Mol Biol* 2000;303:125.
33. Chen HM, You JL, Markin VS, Tsong TY. Kinetic analysis of the acid and the alkaline unfolding states of staphylococcal nuclease. *J Mol Biol* 1991;220:771–778.
34. Chen HM, Markin VS, Tsong TY. Kinetic evidence of microscopic states in protein folding. *Biochemistry* 1992;31:12369–12375.
35. Chen HM, Tsong TY. Comparison of kinetics of formation of helices and hydrophobic core during the folding of staphylococcal nuclease from acid. *Biophys J* 1994;66:40–45.
36. Berman HM, Westbrook J, Feng Z, Gilliland G, Bhat TN, Weissig H, Shindyalov IN, Bourne PE. The Protein Data Bank. *Nucleic Acids Res* 2000;28:235–242. The website of the Protein Data Bank is: <http://www.rcsb.org/pdb/Welcome.do>.
37. Creighton TE. *Proteins: structures and molecular properties*, 2nd ed. New York: W.H. Freeman and Company; 1993. p 177.
38. Shortle D, Ackerman MS. Persistence of native-like topology in a denatured protein in 8M urea. *Science* 2001;293:487–489.
39. Flanagan JM, Kataoka M, Shortle D, Engelman DM. Truncated staphylococcal nuclease is compact but disordered. *Proc Natl Acad Sci USA* 1992;89:748–752.
40. Alexandrescu AT, Shortle D. Backbond dynamics of a highly disordered 131 residue fragment of staphylococcal nuclease. *J Mol Biol* 1994;242:527–546.
41. Alexandrescu AT, Gittis AG, Abeygunawardana C, Shortle D. NMR structure of a stable “OB-fold” sub-domain isolated from staphylococcal nuclease. *J Mol Biol* 1995;250:134–143.
42. Smith LJ, Fiebig KM, Schwalbe H, Dobson CM. The concept of a random coil, residual structure in peptides and denatured proteins. *Fold Des* 1996;1:R95–R106.
43. Kaneshia MI, Tsong T-Y. Dynamics of the cluster model of protein folding. *Biopolymers* 1979;18:1375–1388.
44. Kuwajima K. The molten globule state as a clue for understanding the folding and cooperativity of globular-protein structure. *Proteins* 1989;6:87–103.
45. Chan H-S, Dill KA. Compact polymers. *Macromolecules* 1989;22:4559–4573.
46. Lattman EE, Fiebig KM, Dill KA. Modeling compact denatured states of proteins. *Biochemistry* 1994;33:6158–6166.
47. Kiefhaber T, Baldwin RL. Kinetics of hydrogen bond breakage in the process of unfolding of ribonuclease A measured by pulsed hydrogen exchange. *Proc Natl Acad Sci USA* 1995;92:2657–2661.
48. Kiefhaber T, Baldwin RL. Intrinsic stability of individual α helices modulates structure and stability of the apomyoglobin molten globule form. *J Mol Biol* 1995;252:122–132.
49. Religa TL, Markson JS, Mayor U, Freund SMV, Fersht AR. Solution structure of a protein denatured state and folding intermediate. *Nature* 2005;437:1053–1056.
50. Sallum CG, Martel DM, Fournier RS, Matousek WM, Alexandrescu AT. Sensitivity of NMR residual dipolar couplings to perturbations in folded and denatured staphylococcal nuclease. *Biochemistry* 2005;44:6392–6403.